Magnetic Field-Free Deterministic Switching of a Perpendicular Magnetic Layer by Spin-Orbit Torques

Roberto L. de Orio[a], Siegfried Selberherr[b], and Viktor Sverdlov[a]

[a]Christian Doppler Laboratory for Nonvolatile Magnetoresistive Memory and Logic at the
[b]Institute for Microelectronics, TU Wien, Gußhausstraße 27–29/E360, 1040 Vienna, Austria

ABSTRACT

We demonstrate that a magnetic field-free two-pulse scheme previously proposed to switch an in-plane magnetized free layer is also suitable for switching a perpendicularly magnetized layer. In the case of a symmetric square free layer, deterministic switching is achieved by running the second pulse over a part of the free layer. Applying the same approach to a rectangular free layer results in switching times as short as 0.25 ns. The optimal overlap of the second heavy metal wire with the free layer is found to be between 30-60%. It is shown that the switching scheme yields a large window for the time delay/overlap between the two pulses, still maintaining the switching times as short as 0.25 ns. Consequently, the scheme is extremely robust against pulse duration fluctuations and pulse synchronization failures.

Keywords: Spin-Orbit Torque, Perpendicular Magnetic Layer, Field-Free Switching, Two-Pulse Switching

1. INTRODUCTION

The continuous increase in performance and speed of modern integrated circuits is steadily supported by miniaturization of CMOS devices. However, a rapid increase of stand-by power due to leakages becomes a pressing issue. To reduce the energy consumption, particularly in CPUs, one can replace the SRAM in hierarchical multi-level processor memory structures with a non-volatile memory.[1] The development of an electrically addressable non-volatile memory combining high speed and high endurance is essential to achieve this goal.[2] Spin-orbit torque magnetoresistive random access memory (SOT-MRAM) combines non-volatility, high speed, and high endurance and is thus perfectly suited for applications in caches. However, its development is still hindered by the need of an external magnetic field for deterministic switching of perpendicularly magnetized layers.[3]

In this work we demonstrate that a magnetic field-free two-pulse switching scheme previously proposed[4] to switch an in-plane magnetized free layer (FL) is suitable for switching of a perpendicular layer too. The first pulse is employed to put the magnetization in-plane, while the second pulse pushes the magnetization into a direction, where it starts experiencing the in-plane shape anisotropy field which completes the switching deterministically. In the case of a symmetric layer the deterministic switching is achieved by running the second pulse over a part of the FL to create an in-plane stray magnetic field acting on the rest of the FL. We also demonstrate that the switching scheme is robust with respect to the variations of pulses durations and pulse de-synchronization.

2. SWITCHING SCHEME

The structures of the symmetric square and the rectangular device are shown in Fig. 1. Both structures consist of a perpendicularly magnetized FL grown on top of a heavy metal wire (NM1) of $l = 3\,\text{nm}$ thickness. Another heavy metal wire (NM2) also of $l = 3\,\text{nm}$ thickness lies on top of the FL. The parameters of the FL are listed in Table 1.

The dimensions of the the square structure are $a \times a \times d = 25 \times 25 \times 2\,\text{nm}^3$, while the rectangular device has $a \times b \times d = 52.5 \times 12.5 \times 2\,\text{nm}^3$, where a represents the length, b represents the width, and d is the thickness of the FL. These dimensions, together with the parameters in Table 1, guarantee a thermal stability factor of

Further author information: (Send correspondence to Roberto L. de Orio)
Roberto L. de Orio: E-mail: orio@iue.tuwien.ac.at, Telephone: +43 1 58801 36068

Spintronics XII, edited by Henri-Jean M. Drouhin, Jean-Eric Wegrowe, Manijeh Razeghi, Henri Jaffrès,
Proc. of SPIE Vol. 11090, 110903F · © 2019 SPIE · CCC code: 0277-786X/19/$21 · doi: 10.1117/12.2529119

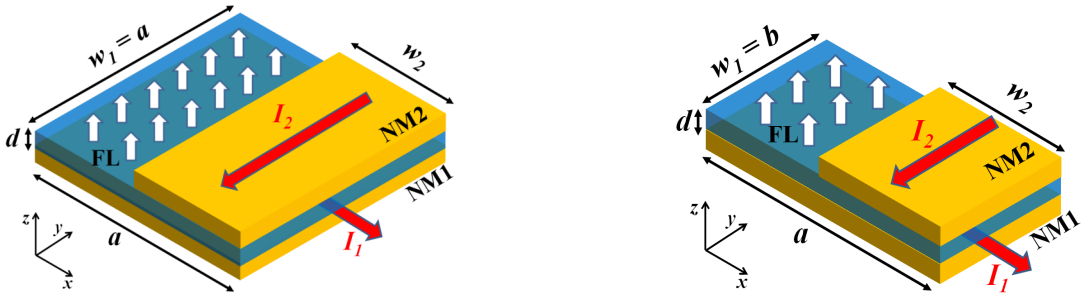

(a) (b)

Figure 1: Two-pulse switching scheme applied to the perpendicularly polarized square magnetic FL. (a) Symmetric square FL with partial overlap of NM2. (b) Rectangular FL with partial overlap of NM2.

Table 1: Parameters used in the simulations.

Saturation magnetization, M_S	4×10^5 A/m
Exchange constant, A	2×10^{-11} J/m
Perpendicular anisotropy, K	2×10^5 J/m^3
Gilbert damping, α	0.05
Spin Hall angle, θ_{SH}	0.3
Free layer dimensions (square)	$25\times25\times2$ nm^3
Free layer dimensions (rectangular)	$52.5\times12.5\times2$ nm^3

about 40, which is sufficient for use in cache memories.[5] As Fig. 1 shows, the FL fully overlaps with the NM1 wire. Thus, the NM1 wire width is $w_1 = 25$ nm for the symmetric and $w_1 = 12.5$ nm for the non-symmetric device. For the symmetric square device, NM2 wire widths (w_2) between 25 nm and 5 nm are simulated. For the non-symmetric rectangular device, $w_2 = 12.5$ nm is used.

The two-pulse switching scheme works as follows: First, a pulse of a fixed duration $T_1 = 100$ ps and a fixed current, $I_1 = 200\,\mu$A for the square and $I_1 = 100\,\mu$A for the rectangular device, is applied through the NM1 wire. This results in a current density of 2.7×10^{12} A/m^2. Then, a second, consecutive perpendicular pulse is applied through the NM2 wire. This pulse yields the same current density (2.7×10^{12} A/m^2) as the first one. However, the second pulse has a variable duration T_2, so the effect of different pulse configurations on the switching dynamics of the device is investigated.

3. MODELING

The magnetization dynamics of the magnetic system is described by the Landau-Lifshitz-Gilbert equation supplemented with the SOT generated by the current pulses acting on the FL, which can be written as

$$\begin{aligned}\frac{\partial \mathbf{m}}{\partial t} &= -\gamma \mathbf{m} \times \mathbf{H_{eff}} + \alpha \mathbf{m} \times \frac{\partial \mathbf{m}}{\partial t} \\ &+ \gamma \frac{\hbar}{2e} \frac{\theta_{SH} I_1}{M_S d w_1 l} \left[\mathbf{m} \times (\mathbf{m} \times \mathbf{y})\right] \Theta(t) \Theta(T_1 - t) \\ &- \gamma \frac{\hbar}{2e} \frac{\theta_{SH} I_2}{M_S d w_2 l} \left[\mathbf{m} \times (\mathbf{m} \times \mathbf{x})\right] \Theta(t - T_1 - \tau) \Theta(T_2 + T_1 + \tau - t),\end{aligned} \tag{1}$$

where $\mathbf{m}$ is the position-dependent magnetization $\mathbf{M}$ normalized by the saturation magnetization M_S, γ is the gyromagnetic ratio, α is the Gilbert damping, and $\mathbf{H_{eff}}$ is an effective magnetic field, e is the elementary charge, $\hbar$ is the Plank constant, θ_{SH} is an effective Hall angle, $\Theta(\cdot)$ is the step function which determines when the pulses are active, and τ is a time delay/superposition between the two current pulses. The effective field $\mathbf{H_{eff}}$ includes the exchange, uniaxial perpendicular anisotropy, demagnetization, and random thermal field at 300 K. To describe the magnetization dynamics, we employ our in-house open-source tool[6] based on the finite difference discretization method. The parameters used in the simulations are given in Table 1.

4. RESULTS

Considering, initially, the square device with a full overlap for the NM2 wire with the FL, i. e. $w_2 = 25\,\text{nm}$, a typical plot of the components of the magnetization vector as a function of time is shown in Figure 2. It shows that the first pulse brings the magnetization from its initial position ($m_z = +1.0$) to the plane of the FL ($m_z = 0$). Then, the second pulse puts the magnetization of the whole FL along the the $-x$ direction ($m_x = -1$). However, after the pulse is removed, the magnetization either returns to the initial $+z$ direction (m_z failed) or flips to the $-z$ direction (m_z flipped), as shown by several realizations of m_z. Thus, some realizations switch and some do not, which is a consequence of the random thermal field.

This is in contrast to the SOT-MRAM cell with a rectangular layer, where the shape anisotropy plays the role of an external magnetic field which drives the magnetization switching after the second current pulse orients the magnetization along the the short side of the rectangle in the $-x$ direction.[4] As the square FL is symmetric and there is no uniaxial shape anisotropy, the switching is unreliable for the full overlap, as shown in Figure 2.

In order to break the symmetry of the squared structure, the width of the NM2 wire is reduced, in such a way that the square FL is only partially covered, which is shown in Figure 1(a). The resulting magnetization dynamics for several values of w_2 is shown in Figure 3, considering $T_2 = 80\,\text{ps}$. It should be pointed out that deterministic switching is observed for all realizations and the switching times are in the range of 0.5 ns to 1.0 ns. For the reduced overlap between the NM2 wire and the FL the switching works as follows: After the magnetization is placed in the plane of the FL by the first current pulse, the SOT due to the second pulse rotates the magnetization only under the NM2 wire and brings it along the x-axis. The magnetization under the NM2 wire creates a stray field which acts as an effective in-plane magnetic field for the rest of the FL. As a consequence, this field causes the magnetization to precess away from its in-plane orientation completing the switching deterministically.

The shortest switching time (taken at the time when $M_Z/M_S = -0.5$) of about 0.6 ns is observed for $w_2 = 10\,\text{nm}$, while the largest switching time, 0.9 ns, is measured for $w_2 = 17.5\,\text{nm}$, the structure with the biggest overlap between the NM2 wire and the FL for which deterministic switching occurs. Considering the structure with $w_2 = 12.5\,\text{nm}$, i.e. 50% overlap between the NM2 wire and the FL, the effect of the second pulse duration (T_2) on the magnetization dynamics is shown in Figure 4. The switching times show a large variation with T_2, being in the range 0.5 ns – 1.5 ns. However, for $T_2 \leq 100\,\text{ps}$ the shortest switching times are obtained. Furthermore, the curves nearly coincide and the switching times are very similar.

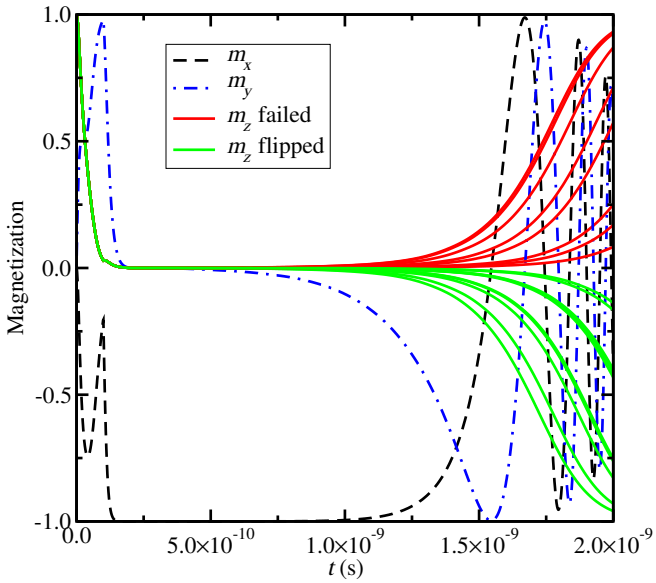

Figure 2: Magnetization components for several realizations for the square structure with $w_2 = 25\,\text{nm}$. The switching is not deterministic, i.e. part of the realizations switches, part does not.

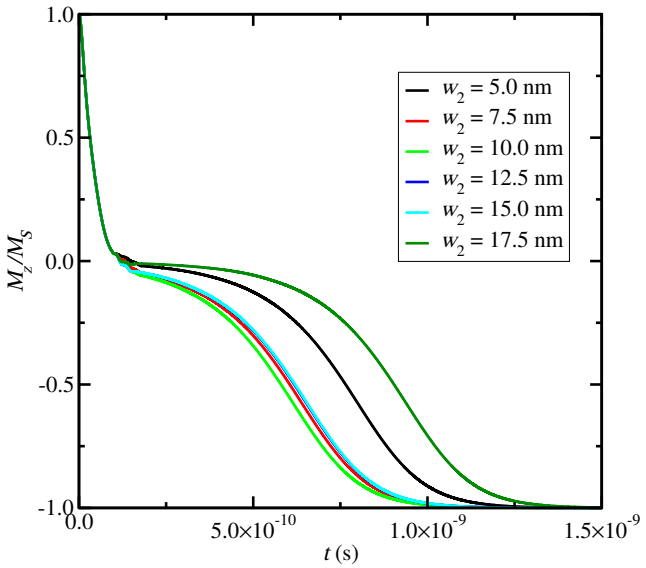

Figure 3: Average z component of the magnetization as a function of time for different overlaps between the NM2 wire and the square FL. The second current pulse has $T_2 = 80\,\text{ps}$.

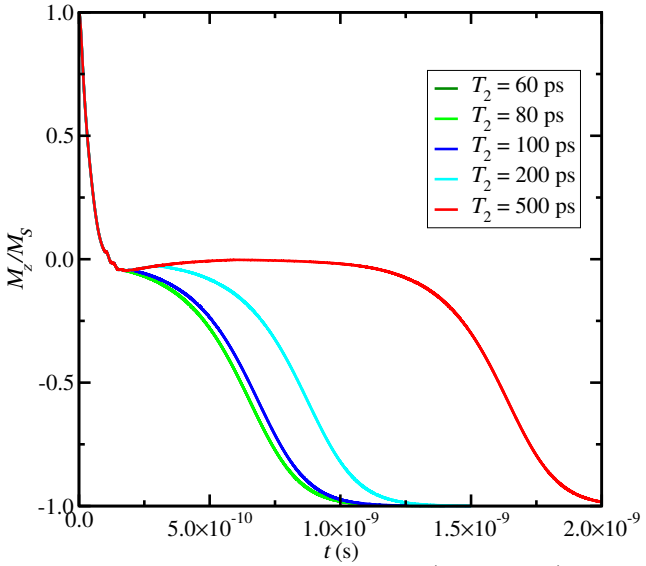

Figure 4: Average of 20 switching realizations for $w_2 = 12.5\,\text{nm}$ (square FL). Reliable switching is observed for all T_2.

Fig. 5 summarizes the switching times as a function of the NM2 wire width, while the second pulse duration is used as parameter. It is interesting to note that the switching times are very close to the minimum value of 0.6 ns for NM2 wire widths in the range $7.5\,\text{nm} \leq w_2 \leq 15\,\text{nm}$ and for pulse durations of $60\,\text{ps} \leq T_2 \leq 100\,\text{ps}$. This shows that an optimal overlap between the NM2 wire and the FL lies around 30% to 60% and, moreover, the switching scheme is very robust with respect to pulse duration fluctuations.

We consider now the rectangular FL device with a reduced NM2 wire width, $w_2 = 12.5\,\text{nm}$, as depicted in Figure 1(b). The resulting switching behavior is shown in Figure 6 together with the curve for the square FL. One can observe a significantly shorter switching time, about 0.25 ns, in comparison to the 0.6 ns switching of the square FL. In the case of the rectangular structure with a smaller overlap between the NM2 wire and the FL, besides the existing shape anisotropy field, the effective field also has a contribution of the stray field in part of the structure. As a consequence, a deterministic, very fast switching occurs.

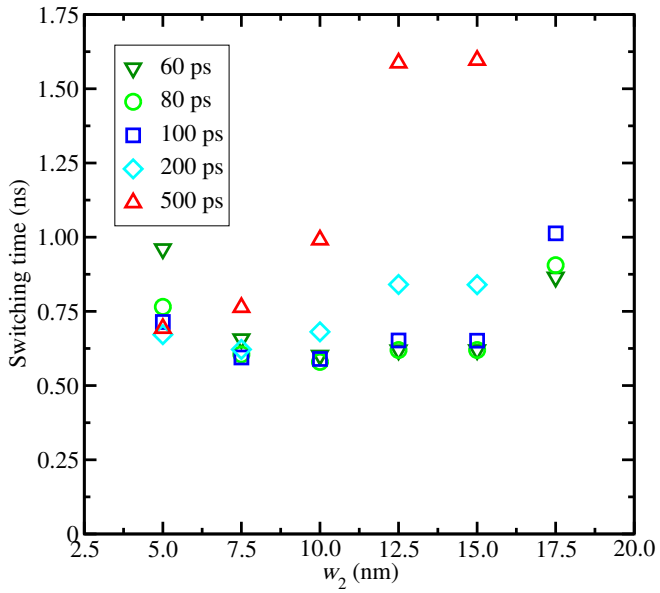

Figure 5: Switching time of the device with the square FL as function of w_2 for several T_2.

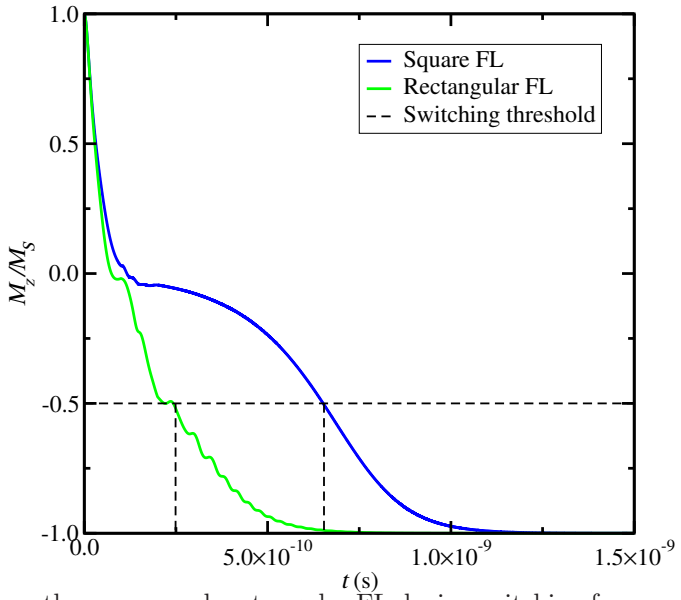

Figure 6: Comparison between the square and rectangular FL device switching for $w_2 = 12.5\,\text{nm}$ and $T_2 = 100\,\text{ps}$.

The above results have considered a perfect synchronization between the two pulses ($\tau = 0$ in Eq. (1)), i.e. the second current pulse starts exactly when the first pulse ends. This is obviously an ideal condition and a time delay or an overlap between the pulses can occur as the signals propagate through the interconnect wires. The effect of the time delay/overlap on the switching of a rectangular FL device with $w_2 = 12.5\,\text{nm}$ and $T_2 = 100\,\text{ps}$ is shown in Figure 7. A negative value of τ represents an overlap between the two current pulses, while a positive value indicates a delay between the end of the first pulse and the beginning of the second one. Also, $\tau = -100\,\text{ps}$ corresponds to a full superposition of the first and the second pulse, i.e. the two pulses occur simultaneously.

Figure 7 shows that sub-0.5ns switching is obtained within the range -50 ps $< \tau <$ 250 ps. Considering that the pulses' width is 100 ps, such a range is indeed very large. Thus, it can be concluded that the scheme is extremely robust against pulse synchronization failures.

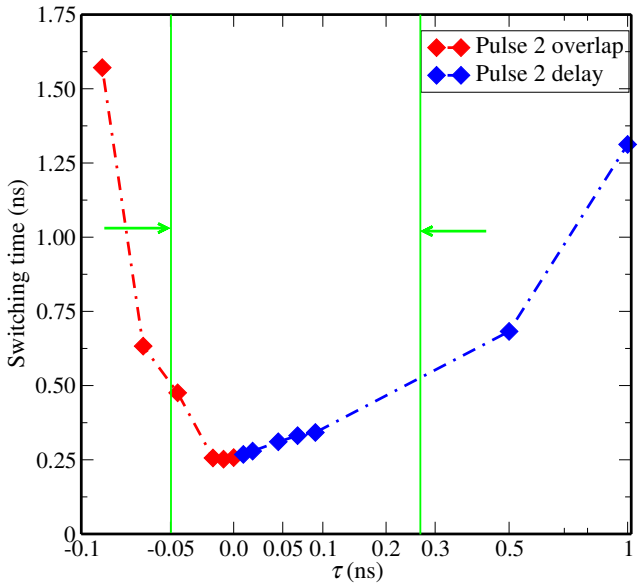

Figure 7: Robust switching at pulse delays between -90 ps $< \tau <$ 1 ns for $w_1 = w_2 = 12.5$ nm (rectangular FL) and equal write pulses ($I_1 = I_2 = 100\,\mu$A, $T_1 = T_2 = 100$ ps). $\tau < 0$ represents an overlap, while $\tau > 0$ corresponds to a delay between the two current pulses.

5. CONCLUSION

Fast (sub-0.5 ns), deterministic, and magnetic field-free switching of a symmetric perpendicularly magnetized recording layer is achieved by employing two orthogonal current pulses (∼100 ps) through two heavy metal lines with a partial overlap with the FL. The optimal overlap lies between 30-60%. For a non-symmetric, rectangular FL switching times as short as 0.25 ns have been demonstrated. Such short times are obtained even in the presence of a large time delay/overlap between the current pulses which drive the device switching. Thus, the scheme is extremely robust against pulse duration fluctuations and pulse synchronization failures.

ACKNOWLEDGMENTS

This work was supported by the Austrian Federal Ministry for Digital and Economic Affairs and the National Foundation for Research, Technology and Development.

REFERENCES

[1] Golonzka, O., Alzate, J.-G., Arslan, U., Bohr, M., Bai, P., Brockman, J., Buford, B., Connor, C., Das, N., Doyle, B., et al., "MRAM as Embedded Non-Volatile Memory Solution for 22FFL FinFET Technology," *Proc. of the 2018 IEDM* , 18.1.1–18.1.4 (2018).

[2] Lee, S.-W. and Lee, K.-J., "Emerging Three-Terminal Magnetic Memory Devices," *Proc. of the IEEE* **104**(10), 1831–1843 (2016).

[3] Baek, S.-H. C., Amin, V. P., Oh, Y.-W., Go, G., Lee, S.-J., Lee, G.-H., Kim, K.-J., Stiles, M. D., Park, B.-G., and Lee, K.-J., "Spin Currents and Spin-Orbit Torques in Ferromagnetic Trilayers," *Nature Materials* **17**, 509–513 (2018).

[4] Sverdlov, V., Makarov, A., and Selberherr, S., "Two-Pulse Sub-ns Switching Scheme for Advanced Spin-Orbit Torque MRAM," *Solid-State Electronics* **155**, 49–56 (2019).

[5] Ikegami, K., Noguchi, H., Takaya, S., Kamata, C., Amano, M., Abe, K., Kushida, K., Kitagawa, E., Ochiai, T., Shimomura, N., et al., "MTJ-Based Normally-Off Processors with Thermal Stability Factor Engineered Perpendicular MTJ, L2 Cache Based on 2T-2MTJ Cell, L3 and Last Level Cache Based on 1T-1MTJ Cell and Novel Error Handling Scheme," *Proc. of the 2015 IEDM* , 25.1.1–25.1.4 (2015).

[6] "ViennaMag." http://www.iue.tuwien.ac.at/software/viennamag/ (2016).